I&EC research
Industrial & Engineering Chemistry Research

pubs.acs.org/IECR
Article

Optimization of the One-Pot Synthesis of Butyl Levulinate from Fructose and 1-Butanol

Roger Bringué,* Rodrigo Soto, Jordi Hug Badia, Eliana Ramírez, Carles Fité, Montserrat Iborra, and Javier Tejero

Cite This: *Ind. Eng. Chem. Res.* 2024, 63, 16701−16709

ABSTRACT: The one-pot synthesis of butyl levulinate from fructose and 1-butanol has been optimized using the ion-exchange resin Dowex 50Wx2 as a catalyst in a batch reactor. The effects of temperature (120−150 °C), initial quantity of water (1-butanol/water molar ratio 1.2−48.5), and fructose (1-butanol/fructose molar ratio 33−77) have been evaluated in order to address the gaps found in the literature. The yield of butyl levulinate is adversely affected by the formation of humins, which is promoted by the presence of water, high temperature, and initial mass of fructose. However, an increase in both the temperature and the mass of fructose has an initial positive effect on the yield. The optimization study concludes that the optimal yield of butyl levulinate is around 140 °C and a 1-butanol/fructose molar ratio of 60. A maximum butyl levulinate yield value of 81.7% is obtained under these conditions after 2 h of run.

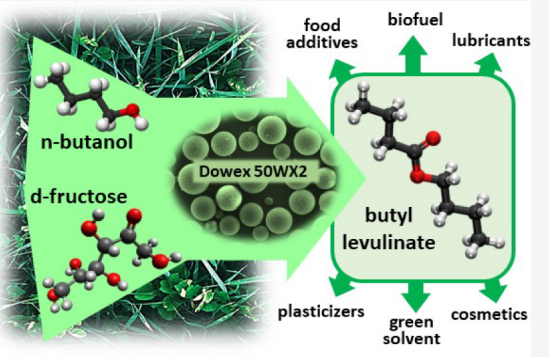

1. INTRODUCTION

The near-future depletion of fossil fuels, along with the pollution and carbon emissions associated with their intensive use by society, has dramatically driven efforts in academia and industry toward the production of bulk platform chemicals and fuels from nonedible renewable biomass.

The transformation of billions of metric tons of biomass produced annually by nature into commodity chemicals or materials, as an alternative to a wide range of oil-based feedstocks, is crucial for sustainability.[1,2] Smart renewable biomass utilization can also be used as a strategy to decrease CO_2 emissions and reduce the use of finite fossil resources.

C_5−C_6 carbohydrates and their derivatives can be produced from cellulose, the main component of lignocellulosic biomass. Levulinate esters (LEs), derived from the dehydration of C_6 sugars into levulinic acid (LA) with 5-hydroxymethylfurfural (5-HMF) as an intermediate, followed by LA alcoholysis using acid catalysts, have attracted much attention as green, high-value-added molecules. They are considered suitable substitutes for traditional fossil fuels due to their energy density (around 30 MJ/L), which is close to that of gasoline (32.4 MJ/L) and higher than that of ethanol (23.5 MJ/L).[3,4] Furthermore, their oxygen content promotes the complete combustion of fuel and reduces particle pollutant emissions.[5,6] Other applications of LEs in daily life include their use as green solvents, polymers, food flavoring agents, cosmetics, foam materials, etc.[7−10]

Methyl, ethyl, and *n*-butyl levulinates are the three LEs most widely studied.[6] Among them, fermentation alcohol-based levulinates are considered 100% biomass-derived compounds, and their use as diesel blend components is of growing interest. Compared to ethyl levulinate, butyl levulinate (BL) enhances conductivity, lubricity, and cold-flow properties.[5] It has a blending cetane number of around 46, close to that of commercial diesel, remains soluble in it at low temperatures,[11−13] and reduces particulate emissions without changing engine power efficiency.[14]

Monosaccharides-derived levulinates esters have significantly higher yields when starting from fructose,[15−17] one of the most direct biomass-derived materials for their production. Open literature about fructose-based butyl levulinate synthesis using acid heterogeneous catalysts is scarce and, in some cases, relevant reaction data about the humins formation, the formic acid/levulinic acid ratio, and the yield of products different from BL are often ignored.[18,19] Fructose butanolysis over $Fe_2(SO_4)_3$ reported a 75% BL yield at 190 °C after 3 h,[20] while it was 16% over Amberlyst 15 at 110 °C after 30 h.[21] Kuo et al.[22] obtained a BL yield of 62.8% using TiO_2 nanoparticles at

Received: April 25, 2024
Revised: September 3, 2024
Accepted: September 9, 2024
Published: September 18, 2024

https://doi.org/10.1021/acs.iecr.4c01580
Ind. Eng. Chem. Res. 2024, 63, 16701−16709

150 °C after 3 h. The use of mesoporous bimetallic catalysts, such as Zr/Al (2)-SB, yielded 72.8% BL at 170 °C after 5 h.[23] The potential of (poly(p-styrene sulfonic acid)-grafted carbon nanotubes (CNT-PSSA) and Amberlyst 15 as catalysts was demonstrated by Liu et al.[24] at 120 °C after 24 h. The BL yields achieved were 87% and 89%, respectively, indicating that acidic ion-exchange resins are promising selective catalysts for this chemical transformation at mild temperatures. In all these works, water-free 1-butanol was used in large excess compared to fructose to shift the system toward BL production and minimize the formation of humins.[25,26] Di Menno Di Bucchianico et al.[27] explored the role of water and GVL as cosolvent on fructose butanolysis kinetics at 110 °C over Amberlite IR120 after 7 h. Water addition (17 wt %) did not improve BL yield (30%), although it promotes the rapid dissolution of fructose even at low temperatures. BL yield increased to 57.5% in the absence of water and 60.4% by adding 30 wt % of GVL in butanol. In a previous work,[28] we studied the feasibility of ion-exchange resins on this reaction using water/1-butanol mixtures in the temperature range 80−120 °C over eight sulfonic polystyrene-DVB ion exchange resins. The process was highly temperature-sensitive, and BL synthesis was highly influenced by the morphology of the acidic ion-exchange resins in the liquid reaction medium. Dowex 50Wx2 gel-type resin showed a 43.4% BL yield at 120 °C after 8h. This low value was attributed to the initial presence of water since water highly inhibits the resin catalytic activity in alcohol media. Interestingly, the BL yield increased to 73.4% when the same experiment was performed with anhydrous butanol under identical conditions.

Given the aforementioned results, it seems clear that there is room for optimization in the production of butyl levulinate from 1-butanol and fructose over Dowex 50Wx2. First, the effect of water should be clarified. Further, the temperature can be increased to check whether a positive effect is observed. Finally, the mass of fructose should be increased for industrial applications, making it ncessary to assess its effect on the production of butyl levulinate. Therefore, in this work, we have focused on the effects of water, temperature, and initial fructose mass on the yield of butyl levulinate, using surface response methodology and subsequent validation to optimize the process.

2. MATERIALS AND METHODS

2.1. Chemicals and Catalyst. 1-Butanol and D-fructose (≥99.5%, Across Organics) were used without further purification. Butyl levulinate (≥98%, Sigma-Aldrich), formic acid (≥98%, Labkem), 5-hydroxymethylfurfural, levulinic acid, butyl formate, and di-*n*-butyl ether (≥98%, Across Organics), as well as deionized water, were used for analysis.

The gel-type ion-exchange resin Dowex 50Wx2 (Aldrich) was used as the catalyst. Its acid capacity is 4.98 mmol H^+/g and its average bead size is 0.105 mm. More detailed information about its textural properties can be found elsewhere.[29]

2.2. Apparatus and Analysis. The setup consisted of a 100 mL stainless steel reactor (Magnedrive II, Autoclave Engineers) heated by an electric oven TC 22 Pro 9, with the temperature controlled to ±0.1 °C using a TOHO TIM-125 TIC controller. The reaction medium was stirred by a magnetic drive turbine equipped with a 4-blade axial-up mixer. The dried catalyst was injected into the reactor from an external cylinder by shifting with N_2.

Liquid samples were taken hourly out of the reactor and analyzed. Butyl levulinate (BL), butyl formate (BF), 5-butoxymethylfurfural (BMF), di-*n*-butyl ether (DBE), and water were determined by gas chromatography (GC). An Agilent HP6890 GC apparatus equipped with a TCD detector and an HP Pona methyl silicone capillary column HP190195−001 (50 m × 0.2 mm × 0.5 μm) analyzed 0.2 μL liquid aliquots. A temperature ramp of 10 °C/min from 50 °C up to 250 °C was initially programmed and then held for 6 min. He (≥99.998%, Linde) was the carrier gas at a column flow rate of 1 mL/min. On the contrary, fructose (F), formic acid (FA), levulinic acid (LA), and 5-hydroxymethylfurfural (HMF) were determined by high-performance liquid chromatography (HPLC). An Agilent 1200 Infinity II HPLC equipped with a refractive index (RI) detector and Agilent Hi-Plex H column (300 × 7.7 mm) analyzed 50 μL of liquid aliquots. The mobile phase was a 0.005 N aqueous solution of H_2SO_4 at a flow rate of 0.6 mL/min and the column temperature 50 °C. Reaction products were identified by an Agilent GC/MS (6890A series GC with an Agilent GC/MS 5973 detector, and chemical database software).

2.3. Procedure. Dowex 50Wx2, in the form of 100−200 mesh beads (0.074−0.149 mm), was used as shipped. The catalyst was dried at 110 °C for 2 h at atmospheric pressure, followed by drying at 10 mbar overnight. The residual water content in the catalyst was less than 3 wt % (Volumetric Karl Fischer Titrator Orion AF8, Thermo Electron Corporation).

Before the catalytic activity runs at different conditions, the fructose solubility in 1-butanol was determined at 25, 80, and 100 °C by a gravimetric method. In each equilibration experiment, solutions of fructose (as shipped) in 1-butanol containing excess visible solids were prepared in 30 mL vials. These were submerged in a thermostatic bath at the desired temperature and stirred using 6 mm wide magnetic stirrers for 48 h to reach solid−liquid equilibrium. Afterward, aliquots of approximately 5 mL were taken from the supernatant liquid and transferred to evaporation vials after filtration using PTFE syringe filters (200 nm mesh). After solvent evaporation, the remaining solid was weighed, and the solubility was computed by mass differences. Three replicates were performed at each temperature, and the final solubility values were expressed as averages. Additionally, the equilibrated solid material at all temperatures was collected by vacuum filtration, dried at room temperature, and characterized by PXRD to confirm that the same solid form was maintained, and that no solution-mediated polymorphic transformations occurred during the equilibration period. The remaining solids formed after solvent evaporation in the weighing vials were also analyzed by PXRD to check the absence of possible soluble impurities originated by the degradation of fructose at higher temperatures. Further information on the gravimetric method used and the procedure for calculating solubility can be found elsewhere.[30]

For the chemical reaction experiments, the reactor was charged with the desired mixture (70 mL), stirred at 500 rpm, set at 2 MPa to ensure a liquid phase throughout the reaction, and heated to the planned temperature. Once the temperature was stabilized, a dried catalyst was injected into the reactor, marking the start of the experiment (time zero). The experiments were conducted for 8 h. The thermal decomposition of fructose during heating was negligible.

The operational conditions were 500 rpm and 2.0 MPa to ensure proper agitation and liquid phase; the temperature range explored was 120−150 °C; the molar 1-butanol to

https://doi.org/10.1021/acs.iecr.4c01580
Ind. Eng. Chem. Res. 2024, 63, 16701−16709

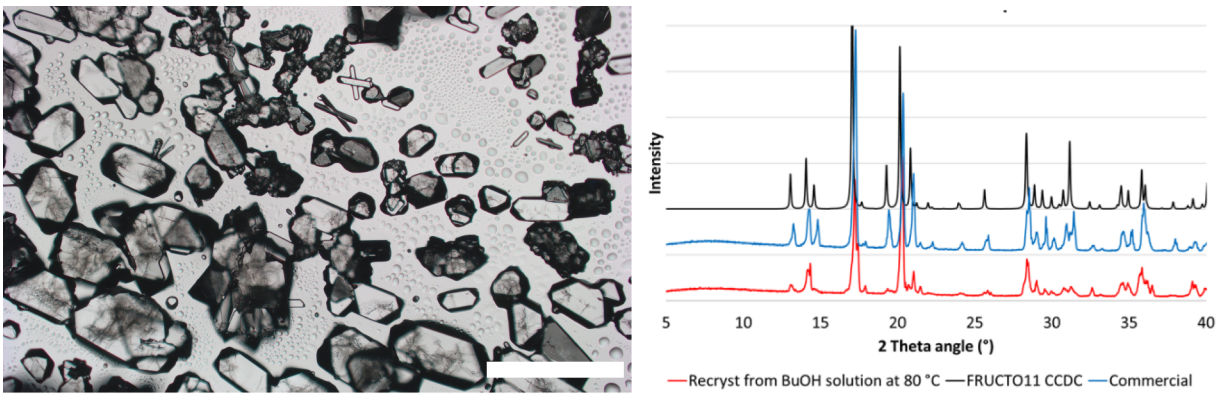

Figure 1. Left: Optical microscope image of fructose as shipped. Scale bar refers to 1 mm. Right: Experimental PXRD pattern of commercial fructose, recrystallized fructose from 1-butanol saturated solution at 80 °C and from CCDC file FRUCTO11.

fructose ratio ($R_{B/F}$) was 37−77; the molar 1-butanol to water ratio ($R_{B/w}$) was 1.2−48.5; the catalyst loading was 1.67−3.3% (1−2 g). Under such operating conditions, the influence of mass transfer was negligible as proved elsewhere.[28]

In each experiment, fructose conversion (X_F), and yield of fructose toward the product j (Y_F^j) are estimated by eqs 1 and 2, respectively

$$X_F = \frac{mole\ of\ F\ reacted}{mole\ of\ F\ initially} \times 100\ [\%,\ mol/mol] \quad (1)$$

$$Y_F^j = \frac{mole\ of\ F\ reacted\ to\ form\ j}{mole\ of\ F\ initially} \times 100\ [\%,\ mol/mol] \quad (2)$$

In order to provide an empirical relationship between operational conditions and yield of BL, a response surface methodology analysis was performed by means of the stepwise procedure considering a second-degree polynomial expression with interaction terms, as follows:

$$y = \beta_0 + \sum_{i=1}^{k} \beta_i x_i + \sum_{i=1}^{k} \beta_{ii} x_i^2 + \sum_{i=1}^{k-1} \sum_{j>i}^{k} \beta_{ij} x_i x_j \quad (3)$$

where y is the response variable, x the independent variables, and β the equation coefficients.

Replicated runs were conducted for some experiments, and the reproducibility of results was found to be reliable. Fructose conversions were accurate within ±1%. On the contrary, BL yields were accurate within ±5% and those of HMF, BMF, and LA within ±5−8%.

3. RESULTS AND DISCUSSION

3.1. Solubility of Fructose. The as-shipped fructose was a white solid chunky crystalline material composed of particles in the range of 100−500 μm (Figure 1 left). The solubility of this material in 1-butanol was experimentally determined at 25, 80, and 100 °C by the gravimetric method described above. The results (Table 1) show that the solubility of fructose in 1-butanol highly increases with temperature. The reproducibility obtained at lower temperatures is very good (0.04−0.045%), indicating the consistency of the followed methodology. Notwithstanding, the value of solubility at 100 °C might be overestimated since it is very close to the melting point of D-fructose (onset at ∼113 °C).[31] At this temeprature, the liquid phase becomes more viscous and paler yellow, typically indicative of the thermal degradation or polymerization of fructose, which significantly hindered the filtration of the supernatant aliquots. Indeed, the kinetics-based interference of fructose's thermal decomposition with its melting temperature has been previously studied.[32]

Table 1. Solubility of Fructose in 1-Butanol

T [°C]	Solubility [g fructose/g butanol]
25	0.00322 ± 0.00001
80	0.04756 ± 0.00002
100	0.40 ± 0.02

Although PXRD is not highly accurate for purity determinations, it can provide a rough approximation to check for the presence of soluble products resulting from fructose degradation in the saturated solutions. Figure 1 (right) shows that the commercial fructose and the recrystallized solids obtained from the filtered butanol-saturated solutions at 80 °C by solvent evaporation both present very similar X-ray diffractograms. Both are consistent with the diffractogram reported for fructose in the FRUCTO11.cif file from the Cambridge Crystallographic Data Centre (CCDC). This result indicates that the degradation of fructose into butanol-soluble products, which could be present in the saturated solutions, was not significant after 48 h at 80 °C. This validates the solubility value obtained at this temperature.

At 80 °C, up to 37.7 g/L of fructose on 1-butanol (2.262 g in 60 mL, $R_{B/F}$ = 52 mol/mol) can be reached. Most of the experiments were carried out at $R_{B/F}$ > 50 and temperature was always higher than 120 °C; therefore, we can ensure that fructose was either completely dissolved or melted as liquid in all tests performed. Furthermore, in all cases some water was present, which is reported to enhance the solubility in the similar system fructose/ethanol.[33]

3.2. Effect of the Initial Amount of Water in the Reaction. The effect of the initial amount of water was examined at 120 °C with an $R_{B/F}$ = 77. Mixtures of 1-butanol and water were prepared in ratios ranging from 60/10 to 70/0 (mL 1-butanol/mL water), corresponding to initial molar ratios, $R_{B/w}$, ranging from 1.2 to 49. The $R_{B/w}$ value of 49 includes the residual water content in both 1-butanol and the catalyst, with no additional water added. The catalyst loading was 1.6%.

Figure 2 shows the evolution of the mole profile for all detected species except water, 1-butanol, and d-*n*-butyl ether, at 120 °C, with $R_{B/F}$ = 77 and two different butanol-to-water

https://doi.org/10.1021/acs.iecr.4c01580
Ind. Eng. Chem. Res. 2024, 63, 16701−16709

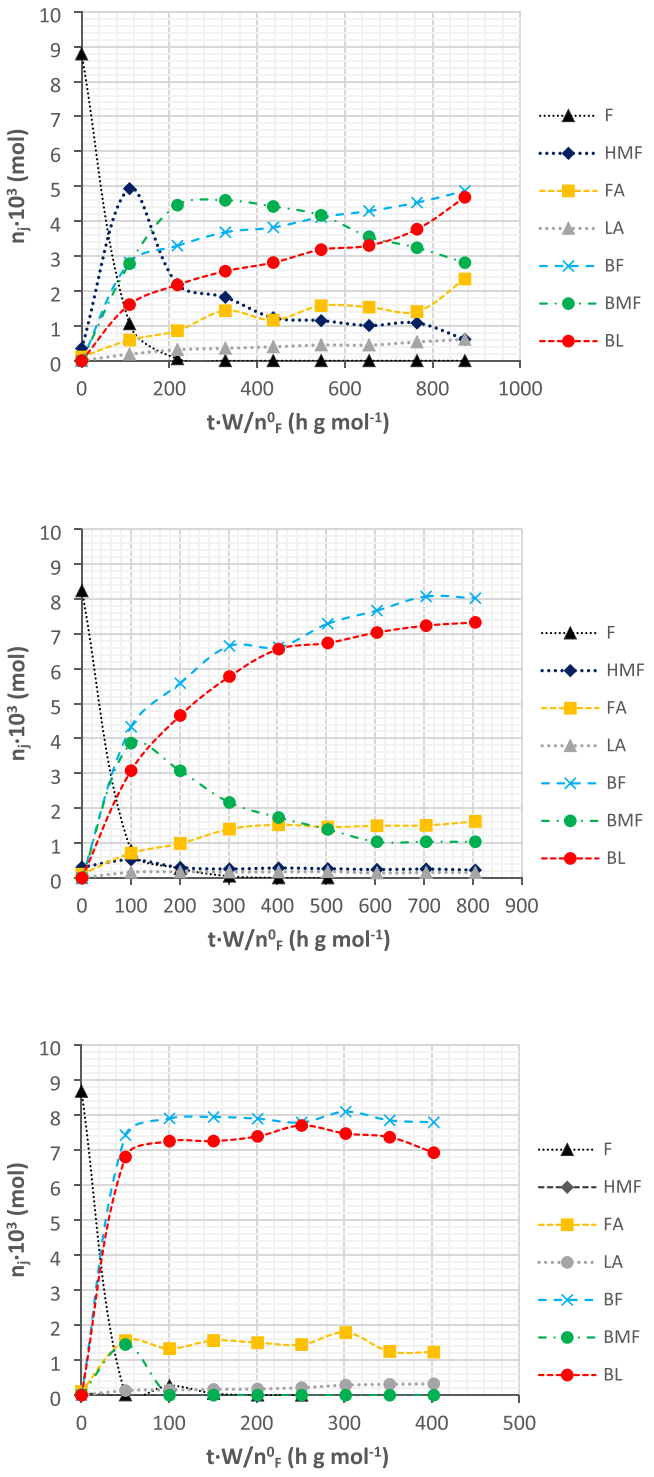

Figure 2. Product distribution mole profile over contact time for the main species: (up) $R_{B/W}$ = 2.4 and T = 120 °C; (middle) $R_{B/W}$ = 49 and T = 120 °C; (down) $R_{B/W}$ = 49 and T = 150 °C. Catalyst load = 1.6 wt %. Dowex 50Wx2, $R_{B/F}$ = 77. Lines are guides to the eye.

ratios, $R_{B/W}$ (Figure 2 up and middle). The trends observed in these plots agree with the reaction scheme shown in Figure 3, which illustrates the complex series-parallel reaction system for producing butyl levulinate from fructose[28,34] wherein the following route key steps can be distinguished:

1) Fructose dehydration reaction to form HMF.
2) Reaction of HMF with 1-butanol to form BMF and its subsequent alcoholysis to BL and BF.
3) HMF rehydration reaction to LA and FA, and subsequent esterification of both acids to BL and BF, respectively.
4) Humins can be formed from fructose and HMF.[35]

As seen in Figure 2, fructose was readily consumed in both runs (contact time 200 h·g·mol^{-1}, time = 2 h), regardless of the initial amount of water. However, water affects the extent of the subsequent reactions: the amount of intermediates HMF and BMF is much lower with a decreased initial quantity of water, while the production of butyl levulinate and butyl formate is favored. As shown in Figure 3, BL can be formed from HMF via the hydrolysis and alcoholysis pathways. The first one includes the formation of LA, while the second includes the production of BMF. As observed, the yield of BMF is higher than that of LA throughout all runs, regardless of the initial amount of water, which is in line with previous observations in the open literature.[27,28] Therefore, it seems that the etherification reaction of HMF with butanol, or alcoholysis, is a faster reaction pathway than its hydration at the temperatures explored with acidic ion-exchange resins catalysts. This effect becomes more pronounced with decreasing initial water content (Table 2).

Interestingly, the amount of humins formed decreased with a lower initial amount of water (see Table 2), and the ratio (FA +BF)/(LA+BL) (mol/mol), shown in Table 2 as the FA/LA ratio. As discussed elsewhere,[28] the excess FA is attributable to the complex reaction network involved in the formation of humins from carbohydrates. Our results confirm the role of water in this network, favoring the formation of humins.[26,27,36] The decrease in humin formation with a lower initial amount of water partly explains the increase in BL production, but not completely. The inhibiting effect of water on ion-exchange resins might also play an important role in the observed activity levels, as noted in other studies.[37−39] Table 2 also shows the conversion of 1-butanol and the yield of dibutyl ether (DBE) at different $R_{BuOH/W}$ ratios. The increase in both magnitudes with decreasing initial water content can also be explained in terms of catalyst activity. The butanol conversion values and DBE yields obtained are consistent with those reported in the literature under comparable conditions.[40]

3.3. Effect of the Temperature. The temperature was increased to 150 °C to assess its effect on activity. As shown in Figure 2 down, the higher temperature accelerates the process as expected but appears to have a minor impact on the maximum quantity of BL that can be obtained under tested conditions, apart from allowing these values to be reached in shorter reaction times (see Figure 4). In 1 h (contact time = 100 h g mol^{-1}), all of the intermediates were already consumed at 150 °C, but the amount of BL produced was similar to that obtained at lower temperatures by the end of the runs.

Table 3 shows the effect of the temperature on the main variables studied at the time when the maximum yield of BL is achieved. Yield of BL increased on increasing temperature from 120 to 130 °C, but then it stabilized around 77% at higher temperatures. This increase can be explained by the total consumption of intermediate species, e.g., HMF and BMF, and also by a slight decrease on the yield of BF. Further, the amount of humins tends to increase with temperature, and also the intermolecular dehydration of n-butanol to the corresponding linear ether, as expected. It is to be noted that

https://doi.org/10.1021/acs.iecr.4c01580
Ind. Eng. Chem. Res. 2024, 63, 16701−16709

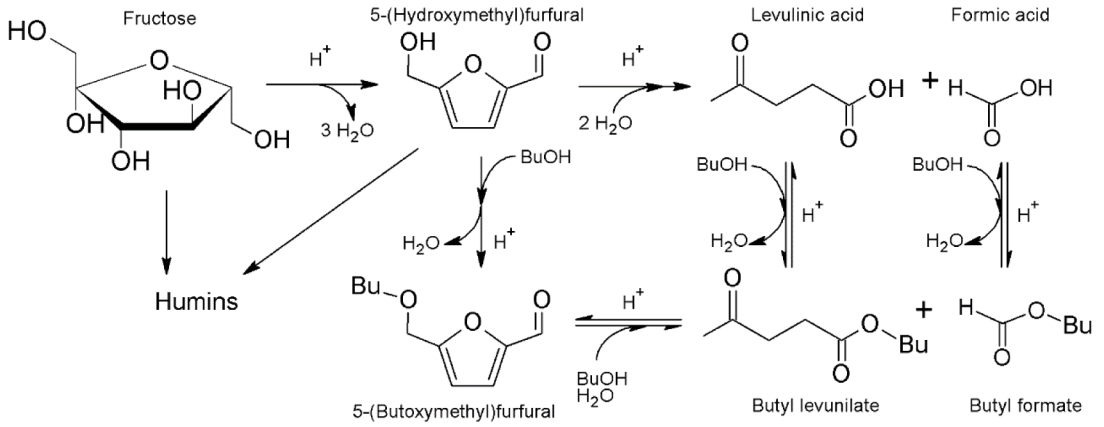

Figure 3. Reaction scheme for butyl levulinate production from fructose and 1-butanol.

Table 2. Main Results Obtained at $R_{B/F}$ = 77 and T = 120 °C on Varying the Amount of Water at t = 8 h[a]

$R_{BuOH/W}$	X_F (%)	Y_F^{HMF} (%)	Y_F^{LA} (%)	Y_F^{BMF} (%)	Y_F^{BL} (%)	Y_F^{FA} (%)	Y_F^{BF} (%)	FA/LA[b] ratio	Humins (%)	X_{BuOH} (%)	Y_{BuOH}^{DBE} (%)
1.2	99.5	3.84	9.72	29.2	32.2	36.4	25.9	1.5	18.5	1.12	----
2.4	100	6.68	6.66	30.5	52.9	25.5	51	1.4	4.2	2.34	0.58
4.7	100	1.95	4.71	16	72.9	23.2	63.7	1.4	11	3.22	1.22
48.5	100	2.26	1.54	10.4	73.4	16.3	80.6	1.3	9.8	4.02	1.93

[a]Catalyst load = 1.6% Dowex 50Wx2. [b](FA+BF)/(LA+BL) molar ratio.

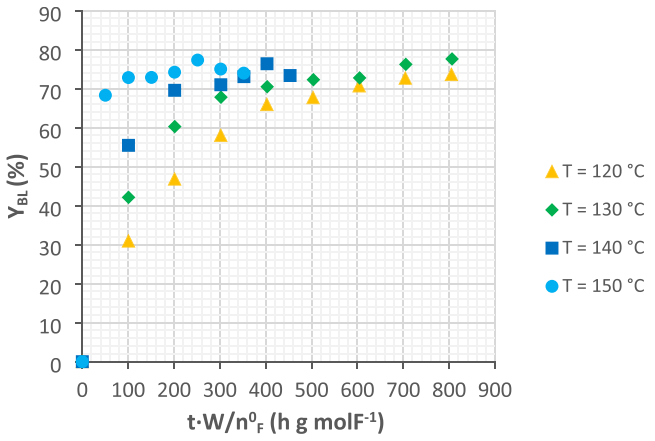

Figure 4. Evolution of the yield of BL with contact time at different temperatures. $R_{B/F}$ = 77, $R_{BuOH/W}$ = 48.5, catalyst load = 1.6% Dowex 50Wx2.

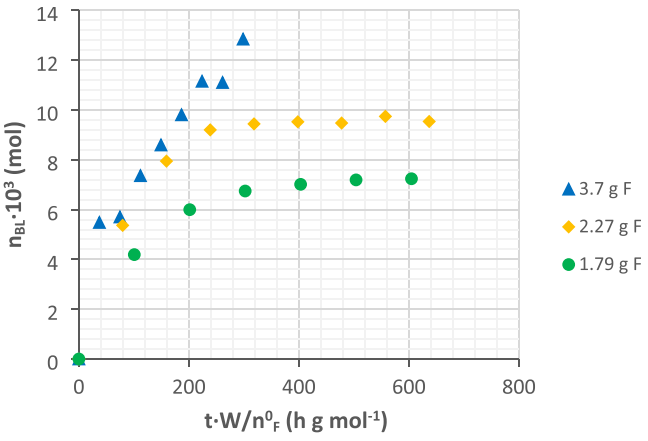

Figure 5. Butyl levulinate mole production over contact time with increasing initial mass of fructose. $R_{BuOH/W}$ = 48.5, catalyst load = 1.6% Dowex 50Wx2, T = 130 °C.

the maximum BL yield is achieved in a shorter reaction time as the temperature increases, which is expected due to the higher reaction rate.

3.4. Effect of Mass of Fructose. The initial concentration of fructose was increased, and its effect on the reactions studied was checked at 130 °C. Three initial fructose concentrations were evaluated, corresponding to initial masses from 1.79 g ($R_{B/F}$ = 77 mol/mol) to 3.7 g ($R_{B/F}$ = 33 mol/mol). As depicted in Figure 5, the evolution of BL mole profiles over the course of the reactions exhibited a noteworthy initial increase, followed by a stabilization phase once all reactants and intermediates were exhausted. Notably, in the run with the highest fructose mass, this stabilization phase was not attained during the entire duration of the experiment. As expected, the

Table 3. Main Results Obtained by Varying the Temperature at the Time When the Maximum BL Yield is Achieved.[a]

T (°C)	t (h)	Y_F^{HMF} (%)	Y_F^{LA} (%)	Y_F^{BMF} (%)	Y_F^{BL} (%)	Y_F^{FA} (%)	Y_F^{BF} (%)	FA/LA ratio	Humins (%)	X_{BuOH} (%)	Y_{BuOH}^{DBE} (%)
120	8	2.26	1.54	10.4	73.4	16.3	80.6	1.29	9.8	4	1.9
130	8	0	1.76	0	77.4	16.8	85.8	1.3	18.8	6.3	4.2
140	4	0	1.52	0	76.4	15.6	77.4	1.26	21	6.5	1.5
150	2.5	0	2.15	0	77.3	14.5	77.2	1.24	24.2	15.6	13.6

[a]$R_{B/F}$ = 77, $R_{BuOH/W}$ = 48.5, catalyst load = 1.6% Dowex 50Wx2.

https://doi.org/10.1021/acs.iecr.4c01580
Ind. Eng. Chem. Res. 2024, 63, 16701−16709

Table 4. Main Results Obtained at 130 °C on Varying the Initial Mass of Fructose, at a Contact Time of 300 h·g·mol·F^{-1}[a]

m^0_F(g)	Y_F^{HMF} (%)	Y_F^{LA} (%)	Y_F^{BMF} (%)	Y_F^{BL} (%)	Y_F^{FA} (%)	Y_F^{BF} (%)	FA/LA ratio	Humins (%)	X_{BuOH} (%)	Y_{BuOH}^{DBE} (%)
1.79	0.3	1.5	14.0	67.8	14.6	75.6	1.30	16.4	6.7	21
2.27	0	1.5	8.3	78.9	16.4	73.7	1.12	20.8	9.6	37.2
3.7	0.0	1.6	8.8	62.2	18.9	64.1	1.3	27.5	8.1	15.0

[a]$R_{BuOH/W}$ = 48.5, catalyst load = 1.6% Dowex 50Wx2.

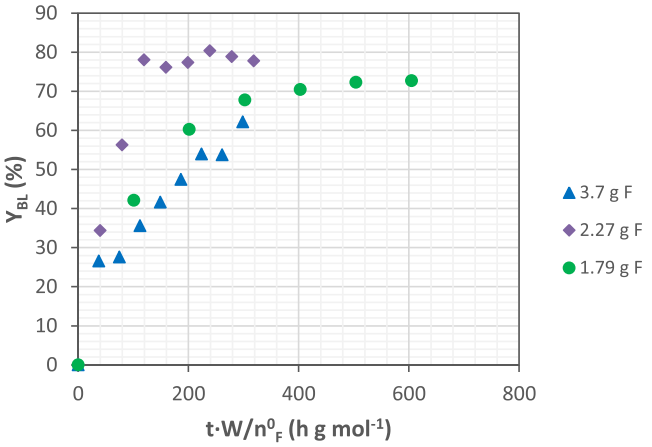

Figure 6. Yield of butyl levulinate over contact time with increasing initial mass of fructose. $R_{BuOH/W}$ = 48.5, catalyst load = 1.6% Dowex 50Wx2, T = 130 °C.

quantity of BL produced at the end of each run increased with the initial fructose mass. However, it is worth mentioning that the formation of humins also increased along with the BL production (Table 4).

Upon examination of the yield of butyl levulinate achieved at the end of the runs with varying initial fructose masses (refer to Figure 6), it becomes evident that the adverse impact of the humin formation reaction becomes pronounced.

For comparison purposes, Table 4 shows the results obtained at the same contact time (300 h·g·mol$_F^{-1}$), which correspond to reaction times from 3 to 6 h, depending on the initial amount of fructose. In all these runs, fructose conversion was complete after 2 h.

As observed in Table 4, the yield of butyl levulinate exhibits an increase as the initial fructose quantity is augmented to 2.27 g. However, this trend reverses when an excess of fructose is introduced. The initial positive effect of the fructose quantity can potentially be attributed to increased catalyst activity, as evidenced by the reduction in the concentration of intermediate compounds. Concurrently, this increase in fructose seems to favor the parallel reaction of butanol dehydration. However, a higher initial amount of fructose, maintaining the mass of catalyst, produces an expected increase of humins, limiting the production of BL.

Considering all of the aforementioned factors and acknowledging that assessing the influence of the initial fructose quantity is not straightforward, it becomes evident that there is an opportunity to explore the optimization of the process.

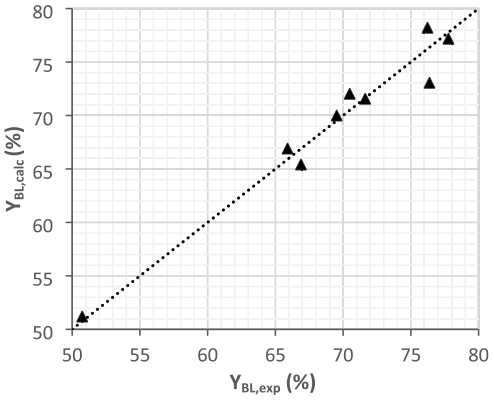

Figure 7. Comparison between experimental and predicted yields of BL.

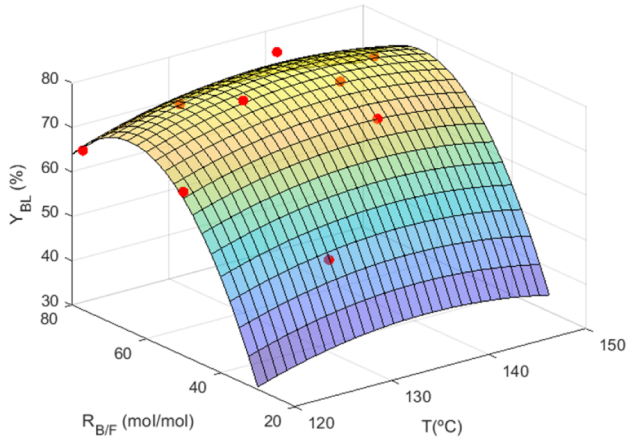

Figure 8. Response surface obtained from the stepwise multivariable regression (eq 4) along with experimental data used in the modeling (red dots).

3.5. Optimization of the Production of BL. In order to maximize the production of BL, some experiments were performed varying the initial fructose concentration and temperature, maintaining the initial amount of extra added water at zero ($R_{B/W}$ = 48.5). The $R_{B/F}$ was studied in the range 37 to 77 at the temperature range of 120 to 150 °C. Four levels for each variable were checked: 37, 50, 60, and 77 for $R_{B/F}$; 120, 130, 140, and 150 °C for the temperature, and t = 4 h was fixed for comparison purposes.

A response surface methodology analysis was used to find the most significant factors that explain Y_{BL} variability. A

Table 5. Results of Stepwise Regression

	β_0	β_1 (T)	β_2 ($R_{B/F}$)	β_3 (T^2)	β_4 ($R^2_{B/F}$)	F_{reg}	R^2	p-Value
Estimate	76.963	1.5434	10.418	−4.6039	−14.326	24.3	0.921	0.00457
SE	1.402	1.323	1.304	2.012	1.892			
p-Value	6.59e−7	0.3083	0.0013	0.0840	0.0016			

https://doi.org/10.1021/acs.iecr.4c01580
Ind. Eng. Chem. Res. 2024, 63, 16701−16709

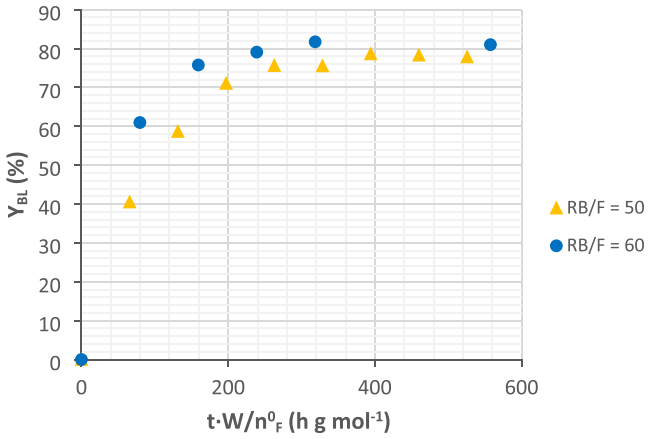

Figure 9. Yield of butyl levulinate obtained over contact time around optimal initial conditions. $R_{BuOH/W}$ = 48.5, catalyst load = 3.2% Dowex 50Wx2, T = 140 °C.

second-degree polynomial was used for the regression, including interaction terms (see eq 3). Independent variables (T and $R_{B/F}$) were coded each to fit the range from −1 to +1. The best empirical model was obtained using stepwise regression methodology: the starting model included an intercept term, linear and squared terms for each predictor, and the product of both predictors; terms were then removed if the p-value of the F-statistic was greater than 0.10. Table 5 lists the parameter estimates, their standard error and p-value, the regression F-statistic, p-value, and the adjusted R^2 for the best model with coded factors. Since the quadratic terms for both factors were statistically significant ($p < 0.10$), linear terms were also considered, although p-value for β_1 is higher than the threshold.

According to the regression results, a second-degree dependence is found between the yield of BL and the two factors, with $R_{B/F}$ having a higher weight. Thus, a rise in reaction temperature ($\beta 1$) and a higher amount of butanol relative to fructose in the reactant mixture ($\beta 2$) both enhance the yield of BL, but a further increase in either variable produces a drop in the observed yield. The interaction term was not statistically significant. The resulting empirical equation predicts data fairly well, as shown in Figure 7.

The derived expression, in terms of uncoded factors, is

$$Y_{BL} = -455.898 + 5.628T + 4.604R_{B/F} - 0.020T^2 - 0.036R_{B/F}^2 \quad (4)$$

From this equation, the corresponding response surface figure can be generated (see Figure 8), which confirms the existence of an optimal region concerning the yield of BL. By differentiating eq 4, we can estimate that the optimal values fall around T = 140 °C and $R_{B/F}$ = 60.

In order to check the performance in the optimal region, additional experiments were performed at 140 °C and $R_{B/F}$ of 50 and 60 but doubling the catalyst mass, with the objective of speeding up the process. The best result was obtained after 2 h of run (contact time ≈320 h·g (mol)$^{-1}$), reaching a BL yield of 81.7% (see Figure 9). This value is among the highest yields of BL ever reported in the open literature. Table 6 compares data of the BL synthesis from fructose found in the literature. It should be noticed that in all these works of water-free 1-butanol is used in large excess compared to fructose. This has the advantage of shifting the system toward BL production

Table 6. Comparison with Literature Data on Butyl Levulinate Synthesis from Fructose and 1-Butanol

Entry	Catalyst	T (°C)	Reaction conditions	Reaction parameters[a]	t (h)	W·t/n^0_F (g·h/mol)	X_F (%)	Y_F^{BL} (%)	Y_F^{BMF} (%)	Observation	Ref.
1	$Fe_2(SO_4)_3$	190	Catalyst 0.1 g Fructose: 0.18 g BuOH: 20 mL Water: 0 mL	$R_{BuOH/F}$ = 217 m_F/W = 1.8 Cat. Load. = 0.6%	3	300	>99	75		Reuse: Y_F^{BL} decreases by 27% after 5 cycles	20
2	Amberlyst 15 Dowex 50Wx8	110	Catalyst 0.65 g Fructose: 0.18 g BuOH: 2g Water: 0 mL	$R_{BuOH/F}$ = 270 m_F/W = 0.28 Cat. Load. = 23%	30	1950	97 97	16 14	71 56		21
3	TiO_2nanoparticles	150	Catalyst 0.2 g Fructose: 0.8 g BuOH: 40 mL Water: 0 mL	$R_{BuOH/F}$ = 98 m_F/W = 4 Cat. Load. = 4.8%	3	135	100	62.8			22
4	Amberlyst 15 CNT-PSSA	120	Catalyst 20 mg Fructose: 50 mg BuOH: 4 mL Water: 0 mL	$R_{BuOH/F}$ = 156 m_F/W = 2.5 Cat. Load. = 0.6%	24	2160	>99 >99	89 87		Reuse: Y_F^{BL} decreases by 18% after 6 cycles	24
5	Amberlite IR120		Catalyst 4.5 g Fructose: 1.6 g BuOH/GVL: 70/30 wt % Water: 0 mL	$R_{BuOH/F}$ = 130 m_F/W = 0.36 Cat. Load. = 3.6%	7	3539	100	60.4	-		27
6	Dowex 50Wx2	120	Catalyst: 1 g Fructose: 1.8 g BuOH: 70 mL Water: 0 mL	$R_{BuOH/F}$ = 79 m_F/W = 1.8 Cat. Load. = 1.7%	8	800	100	73.4	10.4	Humins: 9.8% FA excess[b]: 1.29	28
7	Dowex 50Wx2	140	Catalyst: 2 g Fructose: 2.27 g BuOH: 70 mL Water: 0 mL	$R_{BuOH/F}$ = 60 m_F/W = 1.135 Cat. Load. = 3.3%	2	319	>99	81.7	0	Humins: 12.8% FA excess: 1.2	This work

[a]m_F/W = quotient of fructose to catalyst mass; Cat. Load. = Catalyst loading. [b]FA excess = quotient between the mole of FA + BF produced and those of BL + LA.

https://doi.org/10.1021/acs.iecr.4c01580
Ind. Eng. Chem. Res. 2024, 63, 16701−16709

while simultaneously reducing the humin formation. However, it does have limitations for industrial application. Our result is slightly lower than entry 4, but we reach this value with less than half the ratio of 1-butanol to fructose and in a much shorter reaction time.

4. CONCLUSIONS

The effects of the initial water amount, temperature, and initial fructose mass have been evaluated on the one-pot synthesis of butyl levulinate from fructose and 1-butanol using Dowex 50Wx2. Water inhibits catalyst activity and favors humin formation. Increasing the temperature initially improves butyl levulinate yield within the low-temperature range studied (120−130 °C) and then stabilizes at a consistent value in the higher temperature range (140−150 °C). On the contrary, the temperature increase promotes the formation of humins and dibutyl ether. An increase in the initial mass of fructose initially has a positive effect on the yield of butyl levulinate, but it also promotes the formation of humins, negatively affecting the final outcome. After an optimization study, we estimated that the optimal values in terms of butyl levulinate yield fall around T = 140 °C and a 1-butanol/fructose molar ratio of 60. A maximum butyl levulinate yield value of 81.7% is obtained at these conditions after 2 h of run.

AUTHOR INFORMATION

Corresponding Author

Roger Bringué − *Chemical Engineering and Analytical Chemistry Department, Faculty of Chemistry, Universitat de Barcelona, Barcelona 08028, Spain;* orcid.org/0000-0002-0122-8467; Phone: +34 934021289; Email: rogerbringue@ub.edu

Authors

Rodrigo Soto − *Chemical Engineering and Analytical Chemistry Department, Faculty of Chemistry, Universitat de Barcelona, Barcelona 08028, Spain;* orcid.org/0000-0002-9988-7494

Jordi Hug Badia − *Chemical Engineering and Analytical Chemistry Department, Faculty of Chemistry, Universitat de Barcelona, Barcelona 08028, Spain;* orcid.org/0000-0003-2904-590X

Eliana Ramírez − *Chemical Engineering and Analytical Chemistry Department, Faculty of Chemistry, Universitat de Barcelona, Barcelona 08028, Spain;* orcid.org/0000-0001-8695-1533

Carles Fité − *Chemical Engineering and Analytical Chemistry Department, Faculty of Chemistry, Universitat de Barcelona, Barcelona 08028, Spain;* orcid.org/0000-0003-1361-6026

Montserrat Iborra − *Chemical Engineering and Analytical Chemistry Department, Faculty of Chemistry, Universitat de Barcelona, Barcelona 08028, Spain*

Javier Tejero − *Chemical Engineering and Analytical Chemistry Department, Faculty of Chemistry, Universitat de Barcelona, Barcelona 08028, Spain;* orcid.org/0000-0002-2708-5273

Complete contact information is available at: https://pubs.acs.org/10.1021/acs.iecr.4c01580

Funding

Grant CTQ2014−56618-R from the Spanish Ministry of Economy and Competitiveness is kindly acknowledged.

Notes

The authors declare no competing financial interest.

REFERENCES

(1) Bozell, J. J.; Petersen, G. R. Technology development for the production of biobased products from biorefinery carbohydrates—the US Department of Energy's "Top 10" revisited. *Green Chem.* **2010**, *12*, 539.

(2) Corma, A.; Iborra, S.; Velty, A. Chemical routes for the transformation of biomass into chemicals. *Chem. Rev.* **2007**, *107*, 2411−2502.

(3) Flannelly, T.; Dooley, S.; Leahy, J. J. Reaction Pathway Analysis of Ethyl Levulinate and 5-Ethoxymethylfurfural from d -Fructose Acid Hydrolysis in Ethanol. *Energy Fuels* **2015**, *29*, 7554−7565.

(4) Ghosh, M. K.; Howard, M. S.; Zhang, Y.; Djebbi, K.; Capriolo, G.; Farooq, A.; et al. The combustion kinetics of the lignocellulosic biofuel, ethyl levulinate. *Combust. Flame* **2018**, *193*, 157−169.

(5) Christensen, E.; Williams, A.; Paul, S.; Burton, S.; McCormick, R. L. Properties and performance of levulinate esters as diesel blend components. *Energy Fuels* **2011**, *25*, 5422−5428.

(6) Badgujar, K. C.; Badgujar, V. C.; Bhanage, B. M. A review on catalytic synthesis of energy rich fuel additive levulinate compounds from biomass derived levulinic acid. *Fuel Process. Technol.* **2020**, *197*, 106213.

(7) Govers, F. X. *Solvent refining oil*. US 2,087,473 A, 1937.

(8) Bloom, P. D. *Levulinic acid ester derivatives as reactive plasticizers and coalescent solvents*. US 2010/0216915 A1, 2010.

(9) Rieth, L. R.; Leibig, C. M.; Pratt, J. D.; Jackson, J. *Latex coating compositions including carboxy ester ketal coalescents, methods of manufacture, and uses thereof*. US 9,0740,65 B2, 2015.

(10) Yontz, D. Y. *Fragrant formulations, methods of manufacture thereof and articles comprising the same*. US 2,011,027,464,3 A1, 2011.

(11) Yanowitz, J.; Christensen, E.; McCormick, R. L. *Utilization of Renewable Oxygenates as Gasoline Blending Components*; NREL, 2011.

(12) Joshi, H.; Moser, B. R.; Toler, J.; Smith, W. F.; Walker, T. Ethyl levulinate: A potential bio-based diluent for biodiesel which improves cold flow properties. *Biomass Bioenergy* **2011**, *35*, 3262−3266.

(13) Jenkins, R. W.; Munro, M.; Nash, S.; Chuck, C. J. Potential renewable oxygenated biofuels for the aviation and road transport sectors. *Fuel* **2013**, *103*, 593−599.

(14) Frigo, S.; Pasini, G.; Caposciutti, G.; Antonelli, M.; Maria, A.; Galletti, A. M. R.; et al. Utilisation of advanced biofuel in CI internal combustion engine. *Fuel* **2021**, *297*, 120742.

(15) Démolis, A.; Essayem, N.; Rataboul, F. Synthesis and applications of alkyl levulinates. *ACS Sustainable Chem. Eng.* **2014**, *2*, 1338−1352.

(16) Gautam, P.; Barman, S.; Ali, A. A comparative study on the performance of acid catalysts in the synthesis of levulinate ester using biomass-derived levulinic acid: a review. *Biofuels, Bioprod. Biorefin.* **2022**, *16*, 1095−1115.

(17) Di Menno Di Bucchianico, D.; Wang, Y.; Buvat, J. C.; Pan, Y.; Casson Moreno, V.; Leveneur, S. Production of levulinic acid and alkyl levulinates: a process insight. *Green Chem.* **2022**, *24*, 614−646.

(18) Alamgir Ahmad, K.; Haider Siddiqui, M.; Pant, K. K.; Nigam, K. D. P.; Shetti, N. P.; Aminabhavi, T. M.; et al. A critical review on suitability and catalytic production of butyl levulinate as a blending molecule for green diesel. *Chem. Eng. J.* **2022**, *447*, 137550.

(19) Shan, J.; Wang, Q.; Hao, H.; Guo, H. Critical Review on the Synthesis of Levulinate Esters from Biomass-Based Feedstocks and Their Application. *Ind. Eng. Chem. Res.* **2023**, *62* (42), 17135−17147.

(20) An, R.; Xu, G.; Chang, C.; Bai, J.; Fang, S. Efficient one-pot synthesis of n-butyl levulinate from carbohydrates catalyzed by Fe2(SO4)3. *J. Energy Chem.* **2017**, *26*, 556−563.

(21) Balakrishnan, M.; Sacia, E. R.; Bell, A. T. Etherification and reductive etherification of 5-(hydroxymethyl)furfural: 5-(alkoxymethyl)furfurals and 2,5-bis(alkoxymethyl)furans as potential bio-diesel candidates. *Green Chem.* **2012**, *14*, 1626−1634.

(22) Kuo, C.-H.; Poyraz, A. S.; Jin, L.; Meng, Y.; Pahalagedara, L.; Chen, S.-Y.; Kriz, D. A.; Guild, C.; Gudza, A.; Suib, S. L.

Heterogeneous acidic TiO2 nanoparticles for efficient conversion of biomass derived carbohydrates. *Green Chem.* **2014**, *16* (2), 785−791.
(23) Babaei, Z.; Najafi Chermahini, A.; Dinari, M. Synthesis of n-butyl levulinate as a fuel additive using bimetallic Zr/Al catalysts supported on mesoporous silica: Applying experimental design to optimize the reaction conditions. *Colloids Surf., A* **2021**, *625*, 126885.
(24) Liu, R.; Chen, J.; Huang, X.; Chen, L.; Ma, L.; Li, X. Conversion of fructose into 5-hydroxymethylfurfural and alkyl levulinates catalyzed by sulfonic acid-functionalized carbon materials †. *Green Chem.* **2013**, *15*, 2895−2903.
(25) Hu, X.; Kadarwati, S.; Wang, S.; Song, Y.; Hasan, M. D. M.; Li, C. Z. Biomass-derived sugars and furans: Which polymerize more during their hydrolysis? *Fuel Process. Technol.* **2015**, *137*, 212−219.
(26) Sun, Y.; Sun, K.; Zhang, L.; Zhang, S.; Liu, Q.; Wang, Y.; Wei, T.; Gao, G.; Hu, X. Impacts of Solvents on the Stability of the Biomass-Derived Sugars and Furans. *Energy Fuels* **2020**, *34* (3), 3250−3261.
(27) Di Menno Di Bucchianico, D.; Buvat, J. C.; Mignot, M.; Casson Moreno, V.; Leveneur, S. Role of solvent in enhancing the production of butyl levulinate from fructose. *Fuel* **2022**, *318*, 123703.
(28) Ramírez, E.; Bringué, R.; Fité, C.; Iborra, M.; Tejero, J.; Cunill, F. Assessment of ion exchange resins as catalysts for the direct transformation of fructose into butyl levulinate. *Appl. Catal., A* **2021**, *612*, 117988.
(29) Guilera, J.; Bringué, R.; Ramírez, E.; Iborra, M.; Tejero, J. Synthesis of ethyl octyl ether from diethyl carbonate and 1-octanol over solid catalysts. A screening study. *Appl. Catal., A* **2012**, *413-414*, 21−29.
(30) Soto, R.; Svärd, M.; Verma, V.; Padrela, L.; Ryan, K.; Rasmuson, Å. C. Solubility and thermodynamic analysis of ketoprofen in organic solvents. *Int. J. Pharm.* **2020**, *588*, 119686.
(31) Hurtta, M.; Pitkänen, I.; Knuutinen, J. Melting behaviour of D-sucrose, D-glucose and D-fructose. *Carbohydr. Res.* **2004**, *339*, 2267−2273.
(32) Lee, J. W.; Thomas, L. C.; Schmidt, S. J. Can the thermodynamic melting temperature of sucrose, glucose, and fructose be measured using rapid-scanning differential scanning calorimetry (DSC)? *J. Agric. Food Chem.* **2011**, *59* (7), 3306−3310.
(33) Alavi, T.; Pazuki, G.; Raisi, A. Solubility of Fructose in Water-Ethanol and Water-Methanol Mixtures by Using H-Bonding Models. *J. Food Sci.* **2014**, *79*, 79.
(34) Tian, Y.; Zhang, F.; Wang, J.; Cao, L.; Han, Q. A review on solid acid catalysis for sustainable production of levulinic acid and levulinate esters from biomass derivatives. *Bioresour. Technol.* **2021**, *342*, 125977.
(35) Liu, S.; Zhu, Y.; Liao, Y.; Wang, H.; Liu, Q.; Ma, L.; Wang, C. Advances in understanding the humins: Formation, prevention and application. *Appl. Energy Combust. Sci.* **2022**, *10*, 100062.
(36) Guo, H.; Duereh, A.; Su, Y.; Hensen, E. J. M.; Qi, X.; Smith, R. L. Mechanistic role of protonated polar additives in ethanol for selective transformation of biomass-related compounds. *Appl. Catal., B* **2020**, *264*, 118509.
(37) Pérez-Maciá, M. Á.; Bringué, R.; Iborra, M.; Tejero, J.; Cunill, F. Kinetic study of 1-butanol dehydration to di-n-butyl ether over Amberlyst 70. *AIChE J.* **2016**, *62*, 180−194.
(38) du Toit, E.; Nicol, W. The rate inhibiting effect of water as a product on reactions catalysed by cation exchange resins: Formation of mesityl oxide from acetone as case study. *Appl. Catal., A* **2004**, *277*, 219−225.
(39) Bringué, R.; Ramírez, E.; Iborra, M.; Tejero, J.; Cunill, F. Kinetics of 1-hexanol etherification on Amberlyst 70. *Chem. Eng. J.* **2014**, *246*, 71−78.
(40) Pérez, M. A.; Bringué, R.; Iborra, M.; Tejero, J.; Cunill, F. Ion exchange resins as catalysts for the liquid-phase dehydration of 1-butanol to di-n-butyl ether. *Appl. Catal., A* **2014**, *482*, 38−48.

https://doi.org/10.1021/acs.iecr.4c01580
Ind. Eng. Chem. Res. 2024, 63, 16701−16709